Article
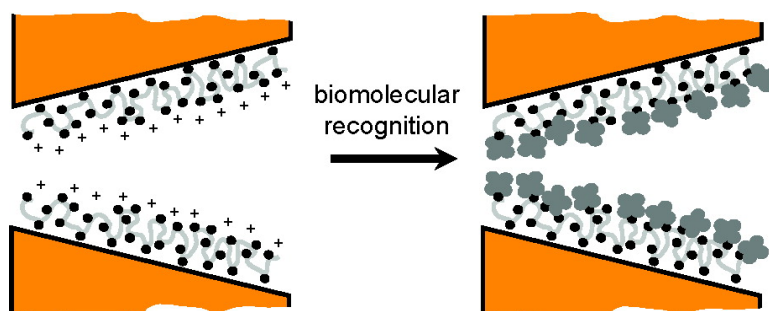
# Biosensing and Supramolecular Bioconjugation in Single Conical Polymer Nanochannels. Facile Incorporation of Biorecognition Elements into Nanoconfined Geometries

Mubarak Ali, Basit Yameen, Reinhard Neumann, Wolfgang Ensinger, Wolfgang Knoll, and Omar Azzaroni

## More About This Article

Additional resources and features associated with this article are available within the HTML version:

- Supporting Information
- Access to high resolution figures
- Links to articles and content related to this article
- Copyright permission to reproduce figures and/or text from this article

**View the Full Text HTML**

# Biosensing and Supramolecular Bioconjugation in Single Conical Polymer Nanochannels. Facile Incorporation of Biorecognition Elements into Nanoconfined Geometries

Mubarak Ali,[†] Basit Yameen,[‡] Reinhard Neumann,[§] Wolfgang Ensinger,[†] Wolfgang Knoll,[‡] and Omar Azzaroni*,[‡,||]

*Technische Universität Darmstadt, Fachbereich Material-u. Geowissenschaften, Fachgebiet Chemische Analytik, Petersenstrasse 23, D-64287 Darmstadt, Germany, Max-Planck-Institut für Polymerforschung, Ackermannweg 10, D-55128 Mainz, Germany, Gesellschaft für Schwerionenforschung (GSI), Planckstr. 1, D-64291 Darmstadt, Germany, and Instituto de Investigaciones Fisicoquímicas Teóricas y Aplicadas (INIFTA), CONICET, Universidad Nacional de La Plata, CC 16 Suc. 4, 1900 La Plata, Argentina*

Received September 8, 2008; E-mail: azzaroni@inifta.unlp.edu.ar

***Abstract:*** There is a growing quest for tailorable nanochannels or nanopores having dimensions comparable to the size of biological molecules and mimicking the function of biological ion channels. This interest is based on the use of nanochannels as extremely sensitive single molecule biosensors. The biosensing capabilities of these nanochannels depend sensitively on the surface characteristics of their inner walls to achieve the desired functionality of the biomimetic system. Nanoscale control over the surface properties of the nanochannel plays a crucial role in the biosensing performance due to the chemical groups incorporated on the inner channel walls that act as binding sites for different analytes and interact with molecules passing through the channel. Here we report a new approach to incorporate biosensing elements into polymer nanochannels by using electrostatic self-assembly. We describe a facile strategy based on the use of bifunctional macromolecular ligands to electrostatically assemble biorecongnition sites into the nanochannel wall, which can then be used as recognition elements for constructing a nanobiosensor. The experimental results demonstrate that the ligand-functionalized nanochannels are very stable and the biorecognition event (protein conjugation) does not promote the removal of the ligands from the channel surface. In addition, control experiments indicated that the electrostatically assembled nanochannel surface displays good biospecificity and nonfouling properties. Then, we demonstrate that this approach also enables the creation of supramolecular multilayered structures inside the nanopore that are stabilized by strong ligand−receptor interactions. We envision that the formation of multilayered supramolecular assemblies inside solid-state nanochannels will play a key role in the further expansion of the toolbox called "soft nanotechnology", as well as in the construction of new multifunctional biomimetic systems.

## Introduction

Ion channels are ubiquitous in nature and represent key elements in many important life processes, such as energy production and storage or signal propagation and processing.[1] The generation of artificial ion channels has strong implications for developing new technologies related to materials and life sciences fields.[2] This explains the increasing interest in incorporating natural transport systems into artificial sensors, which could then exhibit the inherent sensitivity of biochemical systems.[3] However, maintaining a natural environment in an artificial device is a difficult task, demanding the construction of fully and highly functional artificial systems[4] with the ability of mimicking natural systems. This challenging subject led to the creation of different strategies to obtain artificial structures resembling the characteristics of ion channels or nanopores commonly encountered in the membranes of living systems.[5] These structures inspired by their biological counterparts are

[†] Technische Universität Darmstadt.
[‡] Max-Planck-Institut für Polymerforschung.
[§] Gesellschaft für Schwerionenforschung.
[||] Universidad Nacional de La Plata.

(1) (a) Houslay, M. D.; Stanley, K. K. In *Dynamics of Biological Membranes*; John Wiley & Sons: New York, 1982. (b) Robertson, R. N. In *The Lively Membranes*; Cambridge University Press: Cambridge, 1983. (c) Voet, D.; VoetJ. D. In *Biochemistry*; John Wiley & Sons: New York, 1995; Chapter 18, pp 513−537. (d) Perozo, E.; Cortes, D. M.; Sompornpisut, P.; Kioda, A.; Martinac, B. *Nature* **2002**, *418*, 942–948. (e) Sugawara, S.; Sato, H.; Ozawa, T; UmezawaY. In *Frontiers in Biosenorics I: Fundamental Aspects*; Scheller, F. W., Fedrowitz, J., Eds.; Birkhäuser Verlag: Basel, 1997; Chapter 8, pp121–132. (f) Rhee, M.; Burns, M. A. *Trends Biotechnol.* **2007**, *25*, 174–181.

(2) (a) Cross, G. G.; Fyles, T. M.; Montoya-Pelaez, P. J.; van Straaten-Nilenhuis, W. F.; Zhou, X. In *Interfacial Design and Chemical Sensing*; Mallouk, T. E., Harrison, D. J., Eds.; American Chemical Society: Washington, DC, 1994; Chapter 4, pp 38−48. (b) Bailey, H.; Braha, O.; Cheley, S.; Gu, L.-Q. In *Nanobiotechemistry: Concepts, Applications and Perspectives*; Niemeyer, C. M., Mirkin, C. A., Eds.; VCH-Wiley, Weinheim, 2004; Chapter 7, pp 93−112. (c) Tien, H. T.; OttovaA. In *Bioelectrochemistry*; Bard, A. J., Stratmann, M., WilsonG. S., Eds.; VCH-Wiley: Weinheim, 2002; Chapter 16, pp 511−557. (d) Griffiths, *J. Anal. Chem.* **2008**, *80*, 23–27. (e) Kasianowicz, J. J.; Robertson, J. W. F.; Chan, E. R.; Reiner, J. E.; Stanford, V. M. *Ann. Rev. Anal. Chem.* **2008**, *1*, 737–766.

commonly described as "solid-state nanopores" and represent a valuable substitute for fragile lipid bilayer membranes in the case of replacing the biological nanopore with a fully "abiotic" equivalent.[6] Recently, Siwy et al.[7] introduced a new type of protein nanobiosensor made of a single conical gold nanotube embedded within the polymeric membrane, thus creating an asymmetric nanochannel. The sensing read-out consisted of passing an ionic current through the nanochannels. Since the protein analyte and the channel mouth were comparable in size, binding of the protein led to the blocking of the nanochannel, which was detected as a permanent blockage of the ion current.[7]

These experiments clearly revealed the critical role of the pore surface in achieving the desired functionality of the biomimetic system, considering that the chemical groups incorporated on the inner channel walls act as binding sites for different analytes, as well as interacting with molecules passing through the channel.[6,7]

Nanoscale control over the surface properties of the channel wall plays a crucial role in the whole range of applications of solid-state nanochannels.[8−10] In order to achieve this goal

different methods to tailor nanopore surfaces have been developed. One of the most widespread strategies applicable for track-etched pores in polymers was developed by Martin and co-workers and consists of covering the pore walls with gold by electroless deposition followed by the chemisorption of end-functionalized thiols.[11] This procedure enables the incorporation of molecular recognition elements into the inner pore wall of these nanotubes.[12] However, this gold plating step introduces another level of considerable complexity into the pore fabrication process. That is why it is highly desirable to design alternative strategies enabling the facile functionalization of the inner pore wall by directly exploiting the chemical functional groups already existing at the polymer nanochannel wall. For example, in the case of track-etched pores in polyethylene terephthalate (PET) films, the pore surface possesses carboxyl groups.[6f] It would be also very convenient if the method enabled the incorporation of the chemical functionalities in the nano-confined environment without requiring the use of solvents or chemicals that could be harmful or incompatible with the plastic pore wall or biological materials. In this context, considering the inherent surface charge of the pore wall, electrostatic assembly[13,14] could be an extremely versatile route for incorporating chemical functionalities into the nanopore without requiring complex chemical steps. In this work we show that by using simple electrostatic self-assembly we can introduce binding sites into the nanopore, which can then be used as recognition elements for creating a nanobiosensor. Moreover, the possibility of controlling the chemical functionalities and molecular recognition events inside the nanopores enabled facile construction of supramolecular bioconjugates inside the nanochannel.

## Results and Discussion

Single conical nanochannels were prepared as described by Apel et al.[15] using heavy-ion-irradiated PET films. Track-etched pores on PET substrates possess carboxyl groups that are negatively charged under physiological pH conditions (pH 7.4). These moieties can act as sites for the electrostatic assembly of a positively charged building block. Considering that our goal was to electrostatically assemble the biorecognition elements on the pore wall, we created a bifunctional macromolecular multivalent ligand[16] made of biotinylated poly(allylamine) (b-PAH), which was able to interact with the pore surface and

(3) (a) Knoll, W.; Köper, I.; Naumann, R.; Sinner, E.-K. *Electrochim. Acta* **2008**, *53*, 6680–6689. (b) Köper, I.; Schiller, S. M.; Giess, F.; Naumann, R.; Knoll, W. In *Advances in Planar Lipid Bilayers and Liposomes*; Leitmannova Liu, A., Ed.; Academic Press: San Diego, 2006; Vol. 3, Chapter 2, pp 37−53. (c) Sinner, E.-K.; Knoll, W. *Curr. Opin. Chem. Biol* **2001**, *5*, 705–711. (d) Castellana, E. T.; Cremer, P. S. *Surf. Sci. Rep.* **2006**, *61*, 429–444. (e) Jung, S.-Y.; Castellana, E. T.; Holden, M. A.; Yang, T.; Cremer, P. S. In *Nanoscale Assembly: Chemical Techniques*; Huck, W. T. S., Ed.; Springer, New York, 2005; Chapter 6, pp 99−117.

(4) (a) Sisson, A. L.; Shah, M. R.; Bhosale, S.; Matile, S. *Chem. Soc. Rev.* **2006**, *35*, 1269–1286. (b) Jeon, Y.j.; Kim, H.; Jon, S.; Selvapalam, N.; Oh, D. Y.; Seo, I.; Park, C.-S.; Jung, S. R.; Koh, D.-S.; Kim, K. *J. Am. Chem. Soc.* **2004**, *126*, 15944–15945. (c) Leevy, V. M.; Weber, M. E.; Gokel, M. R.; Hughes-Strange, G. B.; Daranciang, D. D.; Ferdani, R.; Gorkel, G. W. *Org. Biomol. Chem.* **2005**, *3*, 1647–1652. (d) Talukdar, P.; Bollot, G.; Mareda, J.; Sakai, N.; Matile, S. *J. Am. Chem. Soc.* **2005**, *127*, 6528–6529.

(5) (a) Li, J.; Gershow, M.; Stein, D.; Brandin, E.; Golovchenko, J. A. *Nat. Mater.* **2003**, *2*, 611. (b) Gershow, M.; Golovchenko, J. A. *Nat. Nanotechnol.* **2007**, *2*, 775. (c) Iqbal, S. M.; Akin, D.; Bashir, R. *Nat. Nanotechnol.* **2007**, *2*, 243. (d) Li, J.; Stein, D.; McMullan, C.; Branton, D.; Aziz, M. J.; Golovchenko, J. A. *Nature* **2001**, *412*, 166. (e) Karnik, R.; Castelino, K.; Fan, R.; Yang, P.; Majundar, A. *Nano Lett.* **2005**, *5*, 1638–1642. (f) Karnik, R.; Fan, R.; Yue, M.; Li, D.; Yang, P.; Majundar, A. *Nano Lett.* **2005**, *5*, 943–948. (g) Daiguji, H.; Yang, P.; Majundar, A. *Nano Lett.* **2004**, *4*, 137–142. (h) van der Heyden, F. H. J.; Bonthuis, D. J.; Stein, D.; Meyer, C.; Dekker, C. *Nano Lett.* **2007**, *7*, 1022–1025. (i) Vlassiuk, I.; Siwy, Z. S. *Nano Lett.* **2007**, *7*, 552–556. (j) White, H. S.; Bund, A. *Langmuir* **2008**, *24*, 2212–2218. (k) Niedema, H.; Vrouenraets, Wierenga, J.; Meijberg, W.; Robillard, G.; Eisenerg, B. *Nano Lett* **2007**, *7*, 2886–2891. (l) Dekker, C. *Nat. Nanotechnol.* **2007**, *2*, 209–215. (m) Savariar, E. N.; Krishnamoorthy, K.; Thayumanavan, S. *Nat. Nanotechnol.* **2008**, *3*, 112–117. (n) Vlassiouk, I.; Park, C.-D; Vail, S. A.; Gust, D.; Smirnov, S. *Nano Lett.* **2006**, *6*, 1013–1017. (o) Kocer, A.; Walko, M.; Meijberg, W.; Feringa, B. L. *Science* **2005**, *309*, 755–758.

(6) (a) Harrell, C. C.; Kohli, P.; Siwy, Z.; Martin, C. R. *J. Am. Chem. Soc.* **2004**, *126*, 15646–15647. (b) Siwy, Z.; Heins, E.; Harrell, C. C.; Kohli, P.; Martin, C. R. *J. Am. Chem. Soc.* **2004**, *126*, 10850–10851. (c) Baker, L. A.; Bird, S. P. *Nat. Nanotechnol.* **2008**, *3*, 73–74. (d) Martin, C.R.; Siwy, Z. *Science* **2007**, *317*, 331–332. (e) Harrell, C. C.; Kohli, P.; Siwy, Z.; C.R.; Martin, *J. Am. Chem. Soc.* **2004**, *126*, 15646–15647. (f) Ali, M.; Schiedt, B.; Healy, K.; Neumann, R.; Ensinger, W. *Nanotechnology* **2008**, *19*, 085713. (g) Harrell, C. C.; Siwy, Z. S.; Martin, C. R. *Small* **2006**, *2*, 194–198. (h) Wharton, J. E.; Jin, P.; Sexton, L. T.; Norne, L. P.; Sherrill, S. A.; Mino, W. K.; Martin, C. R. *Small* **2007**, *3*, 1424–1430. (i) Siwy, Z. S.; Powell, M. R.; Petrov, A.; Kalman, E.; Trautmann, C.; Eisenberg, R. S. *Nano Lett.* **2006**, *6*, 1729–1734. (j) Heins, E. A.; Baker, L. A.; Siwy, S. Z.; Mota, M. O.; Martin, C. R. *J. Phys. Chem. B* **2005**, *109*, 18400–18407. (k) Xia, F.; Guo, W.; Mao, Y.; Hou, X.; Xue, J.; Xia, H.; Wang, L.; Song, Y.; Ji, H.; Ouyang, Q.; Wang, Y.; Jiang, L. *J. Am. Chem. Soc.* **2008**, *130*, 8345–8350.

(7) Siwy, Z.; Trofin, L.; Kohli, P.; Baker, L. A.; Trautmann, C.; Martin, C. R. *J. Am. Chem. Soc.* **2005**, *127*, 5000–5001.

(8) Wanunu, M.; Meller, A. *Nano Lett.* **2007**, *7*, 1580–1585.

(9) Karnik, R.; Castelino, K.; Fan, R.; Yang, P.; Majundar, A. *Nano Lett.* **2005**, *5*, 1638–1642.

(10) Umehara, S.; Pourmand, N.; Webb, C. D.; Davis, R. W.; Yasuda, K.; Karhanek, M. *Nano Lett.* **2006**, *6*, 2486–2492.

(11) Hulteen, J. C.; Jirage, K. B.; Martin, C. R. *J. Am. Chem. Soc.* **1998**, *120*, 6603–6604.

(12) Sexton, L. T.; Horne, L. P.; Martin, C. R. *Mol. BioSyst.* **2007**, *3*, 667–685.

(13) Decher, G. In *Multilayer Thin Films: Sequential Assembly of Nanocomposite Materials*; Decher, G., Schlenoff, J. B., Eds.; Wiley-VCH: Weinheim, 2002; Chapter 1, pp 1−46.

(14) Arys, X.; Jonas, A. M.; Laschewsky, A.; Legras, R. In *Supramolecular Polymers*; Ciferri, A., Ed.; Marcel Dekker: New York, 2000; Chapter 12, pp 505−563.

(15) Apel, P. Y.; Korchev, Y. E.; Siwy, Z.; Spohr, R.; Yoshida, M. *Nucl. Instrum. Methods Phys. Res., Sect. B* **2001**, *184*, 337–346.

(16) (a) Anzai, J.-i.; Kobayashi, Y.; Nakamura, N.; Nishimura, M.; Hoshi, T. *Langmuir* **1999**, *15*, 221–226. (b) Cassier, T.; Lowack, K.; Decher, G. *Supramol. Sci.* **1998**, *5*, 309–315. (c) Lindegren, S.; Andersson, H.; Jacobsson, L.; Back, T.; Skarnemark, G.; Karlsson, B. *Bioconjugate Chem.* **2002**, *13*, 502–509. (d) Kato, N.; Caruso, F. *J. Phys. Chem. B* **2005**, *109*, 19604–19612.
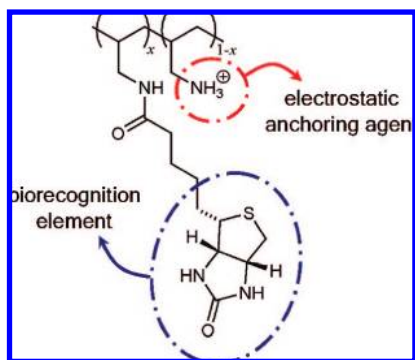
expose the binding sites inside the nanopore without hindering their recognition properties (Scheme 1).

The macromolecular characteristics of the bifunctional polyvalent ligand are due to the fact that having multiple sites, in the same molecule, to electrostatically interact with the pore wall confers the system more stability, enabling the facile functionalization of the pore surface. The nanochannels used in this work were single conical pores in PET, with an opening of only a few nanometers on one side, similar to those which have recently been used successfully for the detection of DNA molecules.[17] These pores were characterized by asymmetric current−potential ($I$−$V$) curves, which originate from the electrostatic interaction between the charged pore surface and the ions passing through them after setting up an electric field across the nanopore-containing membrane.[18] In the case of PET, at neutral pH the pore walls were negatively charged due to ionized carboxyl groups ($COO^-$) (Scheme 2), which in combination with the conical shape of the pore led to an asymmetric intrinsic electrostatic potential along the pore axis, causing different dependencies of the anion and cation concentrations within the pore on the applied voltage.

This effect led to the rectification of the ionic current. As a consequence, the surface charges of the pore wall impacted on the rectifying characteristics of the nanopore and provided insight into the nature of these charges. Figure 1 describes the rectifying characteristics of the PET nanopore prior to and after assembling the bifunctional macromolecular ligand on the pore wall. The $I$−$V$ curves for the $COO^-$-terminated pore surface described a well-defined rectifying behavior, indicating that the nanopore was acting as a rectifier of the ionic transport that preferentially transports species of opposite charges to those on the pore walls.[18]

Assembling the b-PAH led to an immediate reversal of the rectifying characteristics (blue trace in Figure 1), indicating that the electrostatic anchoring promoted the reversal of the preferential direction of ionic transport. As is well-known, the

direction of the rectification is an indicator of the polarity of the charges and the pore walls,[18] and its magnitude depends on the surface charge density. From Figure 1, it can be concluded that the assembly of b-PAH changed the polarity of the nanopore from negative to positive. Moreover, from the magnitude of the rectified currents at +2 and −2 V we can assume that the density of positive charges introduced on the pore surface is comparable to those originally encountered on the negatively charged pore. This change in polarity can be interpreted as a result of the charge overcompensation originating from the assembly of the polycationic multivalent ligand on the negative surface.[19] This phenomenon plays a key role in the electrostatic assembly of polyelectrolyte multilayers in which each polyelectrolyte layer reverses the surface charge of the assembly, enabling the consecutive immobilization of polyelectrolytes bearing opposite charges.[20] The changes in the $I$−$V$ characteristics prior to and after b-PAH assembly allowed the success of the ligand immobilization to be confirmed. We also corroborated that working with different buffered solutions (∼0.1 M in ionic strength) and polarizing the pore at high potential values (∼2 V) do not affect the anchoring of the polyvalent ligands.

Once the pore was functionalized we proceeded to study the biorecognition events inside the solid-state nanopore. In principle, there are three major mechanisms governing the mass transport across nanopores: (a) hydrophobic interactions, (b) electrostatic interactions, and (c) volume exclusion principle.[5h] Regarding hydrophobic interactions, we can mention recent work by Smirnov et al.[5m] in which surface-confined photochromic spyropyran molecules were applied to control the wettability of nanopores in such a way of manipulating the admission of water into the membrane using light as triggering stimulus. A similar approach, in biological membranes, has been also reported by Feringa and co-workers.[5n] On the other hand, when the transport refers exclusively to ionic species, the electrostatic interactions with the charged walls become a crucial variable to tailor the transport characteristics.[6b] In our case, we are mostly dealing with the volume exclusion principle in which the biorecognition event leads to the formation of a ligand−receptor bioconjugate that is supramolecularly confined inside the nanopore. This biorecognition process would affect the effective cross section of the nanopore and have an impact on the flux of the ions through the pore. Consequently, the molecular recognition process would promote a sensitive change on the rectified current passing through the nanopore. It is worth mentioning that the charge of the bioconjugated protein could also affect, at some extent, the electrostatic state of the pore wall and, consequently, contribute of the overall characteristics of the ion transport. However, the bioconjugated protein (∼3 nm) and the pore mouth dimension (∼8 nm) are comparable in size, thus indicating that volume exclusion (changes in effective cross section) would be the major contribution governing the flux through the pore. This assumption is also supported by recent work by Karnik et al.[5e] on the interplay between the competing effect of charge and size of streptavidin on nanochannel conductance. These authors demonstrated that the biomolecule charge dominates at low ionic concentrations, whereas at higher concentrations (as in our case) the volume exclusion effect dominates.[5e]

(17) (a) Mara, A.; Siwy, Z.; Trautmann, C.; Wan, J.; Kamme, F. *Nano Lett.* **2004**, *4*, 497–501. (b) Schiedt, B.; Healy, K.; Morrison, A. P.; Neumann, R.; Siwy, Z. *Nucl. Instrum. Methods Phys. Res., Sect. B* **2005**, *236*, 109–116.

(18) (a) Constantin, D; Siwy, Z. S. *Phys. Rev. E* **2007**, *76*, 041202. (b) Kosińska, I. D.; Goychuk, I.; Kostur, M.; Schmid, G.; Hänggi, P. *Phys. Rev. E* **2008**, *77*, 031131. (c) Liu, Q.; Wang, Y.; Guo, W.; Ji, H.; Xue, J.; Ouyang, Q. *Phys. Rev. E* **2007**, *75*, 051201. (d) Cervera, J.; Alcaraz, A.; Schiedt, B.; Neumann, R.; Ramírez, P. *J. Phys. Chem. C* **2007**, *111*, 12265–12273. (e) Wang, X.; Xue, J.; Wang, L.; Guo, W.; Zhang, W.; Wang, Y.; Liu, Q.; Ji, H.; Ouyang, Q. *J. Phys. D: Appl. Phys.* **2007**, *40*, 7077–7084.

(19) Decher, G. *Science* **1997**, *277*, 1232–1237.

(20) Bertrand, P.; Jonas, A. M.; Lascehwsky, A.; Legras, R. *Macromol. Rapid Commun.* **2000**, *21*, 319–348.

**Scheme 2.** Simplified Depiction of the Incorporation of the Biorecognition Elements into the Single Conical Nanopore[a]
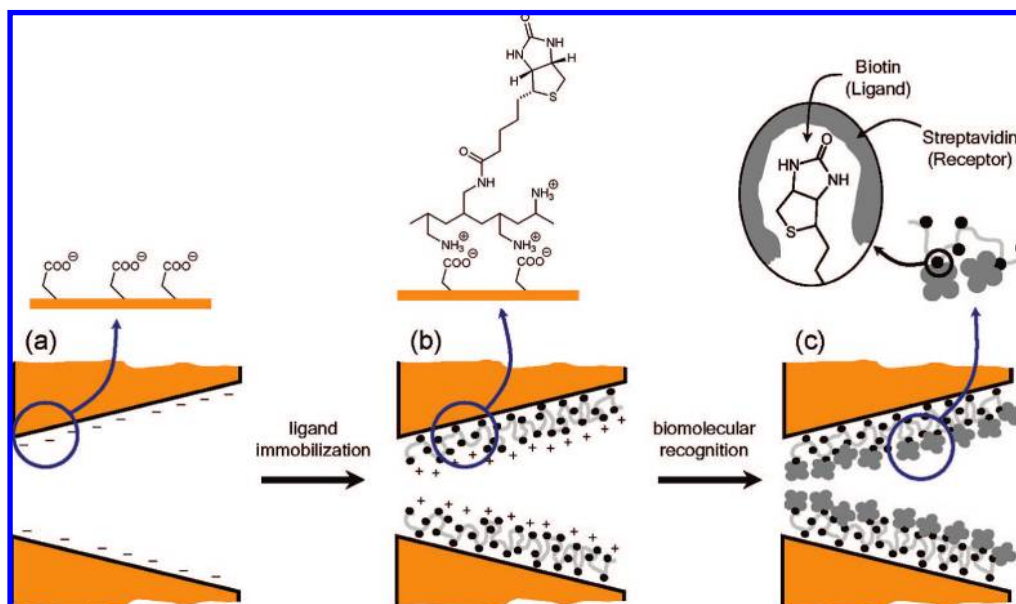


[a] The carboxylate-terminated nanopore (a) is used as a platform for the electrostatic immobilization of the bifunctional macromolecular ligand, b-PAH (b). Then, the biorecognition event proceeds in the presence of the receptor (streptavidin) (c).
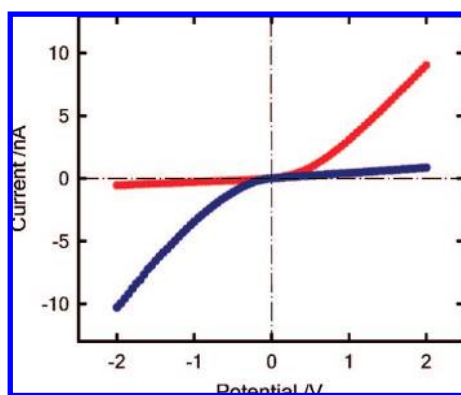


**Figure 1.** Current−voltage characteristics of a single conical nanochannel in 0.1 M KCl prior to (red) and after (blue) the electrostatic assembly of b-PAH.
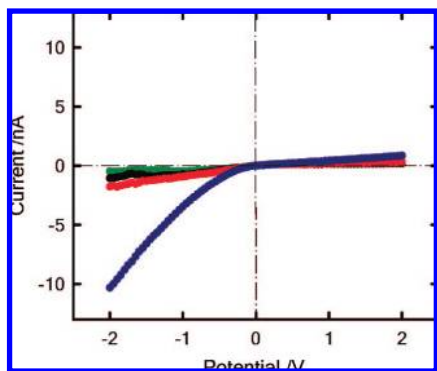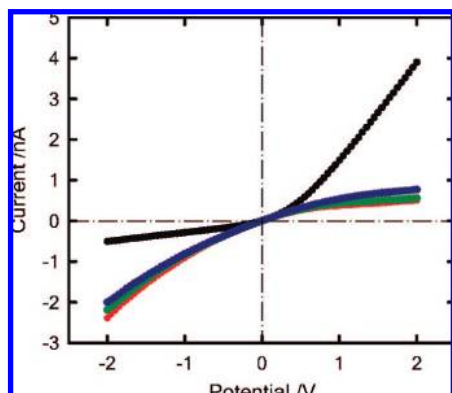


**Figure 2.** Current−voltage characteristics of a b-PAH-modified single conical nanopore in 0.1 KCl in the presence of different concentrations of streptavidin (SAv): (dark blue) no SAv; (red) 1 pM; (black) 10 pM; (green) 100 pM.

Figure 2 describes the changes in the $I-V$ plots upon putting into contact the biotin-modified nanopore with streptavidin solutions of different concentrations. As expected, the presence of streptavidin, even at very low concentrations, led to a drastic

change on the rectified current. The permselective transport of ions across the b-PAH-modified nanopore, measured at −2 V, was −10.3 nA. The presence of 1 pM streptavidin led to a rectified current of −1.7 nA; this means that the blockage of the nanopore due to the formation of the bioconjugate decreased the ionic flux across the nanopore by ∼85%. This effect was even more pronounced when working with more concentrated SAv solutions. The presence of 100 pM SAv promoted a ∼96% decrease of the rectified current observed in the nonbioconjugated nanopore. These experimental results provide clear evidence that the electrostatic assembly enables the anchoring of ligands which are able to biorecognize receptors inside the nanopore, and this biorecognition can be transducted in an electronic signal provided by the ionic flux through the pore.

However, one important aspect of biosensing platforms relies on the selectivity for the detection and transduction of specific events. In other words, in order to show that this approach is valid to create biosensing platforms inside nanopores, it is mandatory to demonstrate that the changes in the rectified current are solely due to the biorecognition event and not to the simple blockage of the nanopore due to the fouling of the protein on the b-PAH-modified PET surface. To verify the bioselectivity of the b-PAH-modified nanopore, we repeated the same experiments using proteins that do not biorecognize biotin, such as lysozyme and bovine serum albumin (BSA), under more concentrated conditions. Figure 3 shows the variations in the $I-V$ plots of b-PAH-modified nanopores in the presence of 100 nM lysozyme and BSA, respectively. From the slight variations in the rectified current, we can conclude that the electrostatically biotinylated nanopores display a remarkable specificity toward streptavidin (Table 1).

These results describing the versatility of the electrostatic assembly to create protein biosensors based on biofunctionalized solid-state nanopores also indicates that this strategy provides a friendly procedure to construct interfacial structures in confined geometries. This constitutes a remaining challenge in materials science related to the creation of functional supramolecular nanostructures derived from the construction of organized
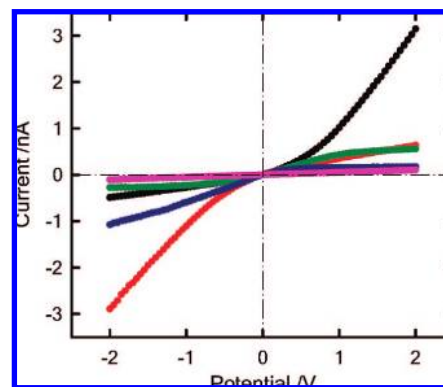
**Figure 3.** Current−voltage characteristics of a single conical nanopore in 0.1 M KCl prior to (black) and after (red) the electrostatic immobilization of b-PAH followed by the addition (separately) of 100 nM lysozyme (green) and 100 nM bovine serum albumin (dark blue).

**Table 1.** Variations on the Rectified Ion Flux in the Presence of the Different Proteins

| protein (concn) | decrease of the rectified current (%) |
| --- | --- |
| streptavidin (1 pM) | ∼ 85 |
| streptavidin (10 pM) | ∼ 90 |
| streptavidin (100 pM) | ∼ 96 |
| bovine serum albumin (100 nM) | ∼ 14 |
| lysozyme (100 nM) | ∼ 9 |

assemblies in nanoconstrained enviroments. Molecular level control of the chemical topology of nanoconfined interfacial structures would be the key to enabling highly functional biomimetic molecular devices.

At this point, we were able to functionalize the pore by using a multivalent bifunctional ligand. After the bioconjugation with the tetravalent streptavidin protein, the pore surface is, in principle, functionalized with a protein that is able to biorecognize biotin centers. This indicates that the chemical/biochemical characteristics of the pore are given by the streptavidin, which could be used for the recognition-mediated spontaneous assembly of a "multivalent" building block, such as the b-PAH. Multivalency is based on interaction through multiple simultaneous molecular contacts[21] and has been demonstrated to be a powerful and versatile self-assembly pathway.[22] Consequently, using the same (ligand−receptor) building blocks, we proceeded to the assembly of the supramolecular bioconjugate inside the nanopore in order to visualize the capabilities of our approach to manipulate the chemical functionalities and structures in nanoconstrained environments (Scheme 3).



**Figure 4.** Current−voltage characteristics of a surface-modified single conical nanopore in 0.1 M KCl corresponding to (black) carboxylate-terminated pore; (red) b-PAH-modified pore; (green) (SAv)(b-PAH)-modified pore; (dark blue) (SAv)(b-PAH)$_2$-modified pore; (pink) (SAv)$_2$(b-PAH)$_2$-modified pore.

We followed the changes occurring in the nanopore through the variations observed in the $I−V$ plots (Figure 4). As described above, the conjugation of the streptavidin on the biotinylated pore led to a decrease of the rectified current. After assembling the polyvalent ligand onto the streptavidin-modified pore, we observed an increase of the rectified current, but the magnitude of this current is still much lower than that detected in the absence of bioconjugation. From the well-defined rectifying characteristics of the $I−V$ plot, we conclude that the recognition-mediated assembly of b-PAH rendered the pore surface positively charged, thus acting as a supramolecular permselective pore transporting preferentially anionic species.

It is worth mentioning that the occurrence of a rectified current probably can be attributed to a reorganization of the interfacial structure after the b-PAH assembly, which affected the effective cross-section area of the nanopore. Even though, subsequent SAv conjugation on the SAv/b-PAH led to an almost complete blockage of the nanopore. This gives clear evidence that the multivalent character of b-PAH enables the creation of a biotinylated interface on top of the SAv layer where the protein is able to biorecognize the ligands without sensitively affecting the stability of the supramolecular structure. More important, in close analogy to polyelectrolyte multilayers, where each polyion is responsible for the reversal of the surface charge, the multivalent character of building blocks is responsible for reversing the ligand−receptor characteristics of the nanopore. This is an important feature of the supramolecular interfacial conjugate[23] in order to create stable and complex functional structures[24] inside the nanochannel. This concept constitutes a

**Scheme 3.** Simplified Depiction of the Formation of a Multilayered Supramolecular Bioconjugate inside the Single Conical Nanopore
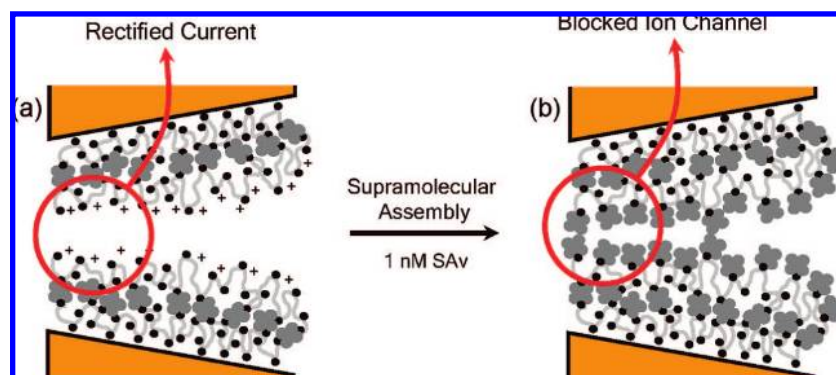
toolbox to achieve actual molecular design of supramolecular systems[25] in nanoconfined environments using predesigned molecular recognition interactions. Supramolecular assembly,[26] the cornerstone of the so-called "soft nanotechnology",[27] occurs spontaneously and can lead to highly functional and controlled structures if selective and directional noncovalent interactions are exploited.[28] The experimental results described above demonstrate that controlling the supramolecular assembly and manipulating the directionality of the processes ocurring into the nanoconfined environment is completely feasible just by using very simple tools.

## Conclusions

In summary, in this work we presented a simple and straightforward strategy to incorporate biorecognition elements in nanoconfined environments, as represented by single conical nanopores. The approach is based on exploiting the ability of a bifunctional multivalent ligand to electrostatically assemble on the charged pore wall and expose the ligand to the inner environment of the nanopore. The experimental results indicated that the electrostatically modified surfaces are very stable and suitable to be used as platforms in biorecognition processes, in which the bioconjugation of the protein does not lead to the removal of the ligands from the surface. Moreover, the electrostatically assembled pore surface displayed good bio-specificity and nonfouling properties as observed in the control experiments using proteins that are not biorecognized by the ligands. Finally, we demonstrated that by using this approach it is possible to exploit the remarkable stability of systems created by ligand−receptor interactions to generate supramo-lecular interfacial structures inside the nanopore.

In this context, we envision that the formation of multilayered supramolecular assemblies inside solid-state nanopores and/or nanochannels could turn into an enabling technology leading to the production of fully artificial biomimetic systems display-ing tailor-made topology, shape, and biochemical functionality.

## Experimental Section

**Materials.** Polyethylene terephthalate (PET) (Hostaphan RN 12, Hoechst) membranes of 12 $\mu$m thickness were irradiated at the linear accelerator UNILAC (GSI, Darmstadt) with single swift heavy ions (Pb, U, and Au) of energy 11.4 MeV/nucleon. Sodium hydroxide (LS Laber-Service, Germany), phosphate-buffered saline (PBS, pH 7.6, Sigma), potassium chloride (Merck, Germany), and fluorescein (FITC)-conjugated streptavidin (Pierce) were used as received.

**Conical Nanopore Fabrication.** The etching method for the fabrication of conical nanopores in PET membranes was developed by Apel et al.[15] Briefly, the heavy-ion-irradiated membrane was placed between both halves of a conductivity cell in which it served as a dividing wall between the two compartments. An etching solution (9 M NaOH) was added on one side and the other side of the cell was filled with stopping solution (1 M HCOOH + 1 M KCl). The etching process was carried out at room temperature. During the etching process, a potential of −1 V was applied across the membrane in order to observe the current flowing through it. The current remains zero as long as the pore is not yet etched through. After the break-through, the stopping solution on the other side of the membranes neutralizes the etchant. The etching process was stopped when the current was reached a certain value, and the pore was washed first with stopping solution in order to quench the etchant, followed with deionized water. The etched membrane was immersed in deionized water in order to remove the residual salts. After etching, the diameter of the large opening ($D$) of the pore was determined by scanning electron microscopy (SEM) using a PET sample containing $10^7$ pores/cm$^2$ that was etched simulta-neously with the single pore under the same conditions. The diameter of the small opening ($d$) was estimated from its conductiv-ity by the following relation:[15]

$$d = \frac{4LI}{\pi D \kappa V}$$

where $L$ is the length of the pore, which could be approximated to the thickness of the membrane; $d$ and $D$ are the small and large opening diameter of the pore, respectively; $\kappa$ is the specific conductivity of the electrolyte (1 M KCl), $V$ is the voltage applied across the membrane, and $I$ is the measured current. The conical nanopores used in our studies had a small opening (tip) with a diameter of 7−10 nm and a large opening (base) with a diameter of 450−550 nm. On average, the assembly of the polyvalent ligand and the bioconjugation of the protein led to a tip diameter decrease of 1−2 and 3−4 nm, respectively.

**Current−voltage Measurements.** The membrane containing the single conically nanopore was mounted between the two halves of the conductivity cell, and both halves of the cell were filled with phosphate-buffered saline (pH = 7.6) prepared in 0.1 M KCl solution. A Ag/AgCl electrode was placed into each half-cell solution, and a Keithley 6487 picoammeter/voltage source (Keithley Instruments, Cleveland, OH) was used to apply the desired transmembrane potential in order to measure the resulting ion current flowing through the nanopore by applying a scanning triangle voltage from −2 V to +2 V on the tip side while the base side of the pore remain connected to the ground electrode.

**Synthesis of Biotinylated Poly(allylamine) Hydrochloride.** 6-Biotinyl-*N*-hydroxysuccinimide ester[29] (0.41 g, 1.26 × 10$^{-3}$ mol) was dissolved in 3 mL of DMF by heating to 80 °C. The solution was cooled to room temperature and was added dropwise to a solution of 0.5 g of PAH (MW ~15,000) solution in 3 mL of aqueous PBS buffer containing 0.13 g of NaHCO$_3$ (1.575 × 10$^{-3}$ mol, 1.5 equiv of biotin-NHS). The clear solution obtained was

(21) (a) Kane, R. S. *AlChE J.* **2006**, *52*, 3638–3644. (b) Kiessling, L. L.; Gestwicki, J. E.; Strong, L. E. *Angew. Chem., Int. Ed.* **2006**, *45*, 2348–2368.

(22) (a) NiemeyerC. M. In *Nanobiotechnology: Concepts, Applications and Perspectives*; Niemeyer, C. M.,; Mirkin, C. A., Eds.; Wiley-VCH: Weinheim, 2004; Chapter 15, pp 227−243. (b) Mulder, A.; Huskens, J.; Reinhoudt, D. N. *Org. Biol. Chem.* **2004**, *2*, 3404–3424. (c) Crespo-Biel, O.; Ravoo, B. J.; Reinhoudt, D. N.; Huskens, J. *J. Mater. Chem.* **2006**, *16*, 3997–4021.

(23) (a) Azzaroni, O.; Mir, M.; Álvarez, M.; Tiefenauer, L.; Knoll, W. *Langmuir* **2008**, *24*, 2878–2883. (b) Azzaroni, M.; Mir; Knoll, W. *J. Phys. Chem. B* **2007**, *111*, 13499–13503. (c) Knoll, W.; Liley, M.; Piscevic, D.; Spinke, J.; Tarlov, M. J. *Adv. Biophys.* **1997**, *34*, 231–251.

(24) Schmittel, M.; Kalsani, V. In *Functional Molecular Nanostructures*; Schlüter, A. D., Ed.; Springer: Heidelberg, 2005;) Chapter 1, pp 1−54.

(25) (a) Knoll, W.; Park, H.; Sinner, E.-K.; Yao, D.; Yu, F. *Surf. Sci.* **2004**, *570*, 30–42. (b) Ringsdorf, H.; Wüstefeld, R. *Phil. Trans. R. Soc. London A* **1990**, *330*, 95–108. (c) Muller, W.; Ringsdorf, H.; Rump, E.; G. Wildburg; Zhang, X.; Angermaier, L.; Knoll, W.; Liley, M.; Spinke, J. *Science* **1993**, *262*, 1706–1708. (d) Takami, T.; Delamarche, E.; Michel, B.; Gerber, Ch.; Wolf, H.; Ringdorf, H. *Langmuir* **1995**, *11*, 3976–3881. (e) Steinbeck, M.; Ringsdorf, H. *Chem. Commun.* **1996**, 1193–1194.

(26) (a) Liu, G.-Y; Amro, N. A. *Proc. Nat. Acad. Sci. U.S.A.* **2002**, *99*, 5165–5170. (b) Hartgerink, J. D.; Beniash, E.; Stupp, S. I. *Science* **2001**, *294*, 1684–1688. (c) Martín, T.; Obst, U.; Rebek, J., Jr *Science* **1998**, *281*, 1842–1845.

(27) (a) Huck, W. T. S. *Mater. Today* **2008**, *11*, 24–32. (b) Jones, R. A. L. *Soft Machines: Nanotechnology and Life*; Oxford University Press: New York, 2004; Chapter 5, pp 88−125.

(28) Yokoyama, T.; Yokoyama, S.; Kamikado, T.; Okuno, Y.; Mashiko, S. *Nature* **2001**, *413*, 619–621.

(29) Wilchek, M. *Methods in Enzymology*; Academic Press: San Diego, 1990; Vol. 184.

allowed to stir at room temperature for 24 h and was subjected to dialysis against water for 5 days (dialysis membrane cutoff was 3500). The aqueous solution was lyophilized to give biotinylated poly(allylamine) hydrochloride (b-PAH) as a white solid. The content of biotin was determined by $^1$H NMR and was found to be 21%.

**Electrostatic Self-Assembly of b-PAH inside the Nanochannel.** As a result of the etching procedure carboxylic acid moieties appear on the surface of the PET nanochannel, thus resulting in a negatively charge surface. The polycation, b-PAH (bifunctional polyvalent ligand), was electrostatically self-assembled on the negatively charged surface of the conical nanochannel while the membrane was still mounted on the electrochemical cell used for $I-V$ measurements. An aqueous solution of b-PAH (1 mg/mL) was placed on both sides of the track-etched polymer membrane and allowed to self-assemble during overnight. Then, the membrane was washed three times with Milli-Q water and three times with PBS buffer (pH 7.6) solution prior to biosensing experiments. The current−voltage curves of biotinylated nanochannels were measured with 0.1 M KCl as electrolyte (buffered with PBS, pH 7.6). The

various concentrations of streptavidin prepared in the same electrolyte were used for the respective $I-V$ measurements.

**Formation of a Multilayered Supramolecular Bioconjugates inside the Nanochannel.** The SAv solution (1 nM) was placed on both sides of the b-PAH-functionalized PET nanochannel for 4 h, and the $I-V$ curve was measured. The SAv solution was then replaced with b-PAH solution and allowed to self-assemble on the SAv layer overnight. After washing three times with Milli-Q water and three times with PBS solution, 1 nM SAv was introduced again on both sides of the nanochannel for 4 h, and a new $I-V$ curve was measured.